Three-Stage Character of Strain Hardening of α-Ti in Tension Conditions

A Roth, K E K Amouzou, M A Lebyodkin, T Richeton, T A Lebedkina, J.S. Lecomte

Three-stage character of strain hardening of a-Ti in tension conditions

A. Roth*, K.E.K. Amouzoua, M.A. Lebyodkin*, T. Richeton, T.A. Lebedkina and J.S. Lecomte

Laboratoire d'Etudes des Microstructures et de Mécanique des Matériaux (LEM3), UMR 7239, CNRS / Université de Lorraine, Ile du Saulcy, 57045 Metz Cedex 01, France

amandine.roth@univ-lorraine.fr, mikhail.lebedkin@univ-lorraine.fr

Keywords: Titanium, Tension, Twinning, Strain hardening, Anisotropy, EBSD, Modeling

Abstract.

The plasticity of hexagonal materials is strongly anisotropic and involves different microscopic mechanisms such as mechanical twinning and dislocation glide. Twins are often considered to be responsible for a particular three-stage shape of compression curves, unusual for polycrystals with cubic structure. However, the role of twins remains a matter of debate and it is not clear if the same features appear in other testing conditions. We performed tensile tests on commercially-pure Ti samples cut along the rolling and the transverse direction, which yielded several unexpected results. In particular, the work hardening rate was found to be lower in the latter case, although the EBSD measurements revealed for them a larger volume fraction of twins. Also, the two kinds of specimens showed an opposite sign for the strain-rate effect on the proneness to the three-stage shape of the deformation curves. As a first approach, these observations are compared to the results derived from a simple Kocks-Mecking model. The possible role of twinning and dislocation glide on the anisotropy of mechanical behavior of titanium is then discussed.

Introduction

At ambient temperature, titanium has a hexagonal close-packed (hcp) structure which is characterized by high anisotropy of mechanical properties with regard to crystallographic directions. The plastic deformation of hcp metals implies indeed twinning in addition to the activation of slip systems with different glide resistance. The role of twinning strongly varies between different hcp materials, in relation with the c/a ratio of the axes of the hexagonal elementary cell. For example, Mg is known to show much more intense twinning than Ti. However, hcp materials manifest many similar mechanical properties, e.g., an asymmetry of the yield stress with regard to the stress sign and material texture, a high work hardening rate, and, sometimes, an unusual concave shape of compression curves (see, e.g., [1]). These peculiarities are often considered from the viewpoint of twinning but remain however a matter of controversy. Many authors discuss that twin boundaries acting as barriers to dislocations glide, likewise grain boundaries, can contribute to an increase in the flow stress. This suggestion is however not as obvious at it could seem (see, e.g., [2]), considering other aspects of the effect of twinning, e.g., facilitation of dislocation glide because of the reorientation of the lattice inside twins. Even more debate has been devoted to strain hardening behavior of hcp materials. An often reported feature found for various materials consists in a three-stage character of compression curves [1,3-6]. More precisely, the initial stage A characterized by a decreasing strain hardening rate $\Theta = d\sigma / d\varepsilon^p$ is followed by an

increase in Θ (stage B) and, finally, a new decrease (stage C). Several distinct points of view on the mechanisms responsible for these variations were discussed in the literature. Taking into account the strong texture, Kailas et al. suggested an analogy with the

well-known hardening stages of single crystals, thus ascribing the three stages observed in CP-Ti, respectively, to easy glide, multiple dislocations slip, and dynamic recovery [3]. Nemat-Nasser et al. suggested that the stage B in CP-Ti could be ascribed to dynamic strain aging of dislocations, caused by their interaction with solute atoms [4]. Nevertheless, this explanation does not apply to ambient temperature because the dynamic strain aging is only essential in Ti in the temperature range of 500–850 K, as shown in [5]. Salem et al. [6,7] performed an elaborated investigation of plasticity of pure Ti in relation to microstructure changes and ascribed the stage A to the usual dynamic-recovery regime observed in metals with a high stacking fault energy, the stage B to the effect of twins on the resistance to dislocation glide, and the stage C to saturation of the twin volume fraction. So far, it is not clear whether the conclusion on the three-stage nature of plastic deformation may also be relevant in tension. The present work aims at characterizing the mechanical anisotropy of commercially pure (CP) Ti and especially its strain hardening behavior in tensile conditions.

Experimental measurements

Deformation curves. The as-received CP-Ti sheet (T40) with the composition given in [8] had an average grain size around 9 μm. The samples with a gage section of 30×7×1.62 mm3 were cut parallel to either the rolling direction (hereinafter referred to as RD-samples) or the transverse direction (TD-samples). The specimens were deformed at room temperature at a constant crosshead velocity corresponding to initial applied strain rates $\dot{\varepsilon}_a$ ranging from 5×10^{-5} s^{-1} to 8×10^{-3} s−1. A sensor arm extensometer was applied to obtain high-accurate true strain-true stress curves. Two to four samples were tested for each strain rate and each kind of sample orientation, and displayed very good reproducibility. Examples of deformation curves are shown in Fig.1. In the inset of Fig.1, it is seen that the yield stress obeys linear dependencies on the logarithmic applied strain rate with higher values for TD-samples. Such behavior is ordinarily related to thermally activated dislocation motion and is thus consistent with the data which indicate that twinning only starts after accumulation of some deformation [6,7]. The slopes of the dependencies are not equal for two specimen orientations. Together with the difference in the yield stress value, the last observation indicates that different slip systems must govern the onset of plasticity in each case.

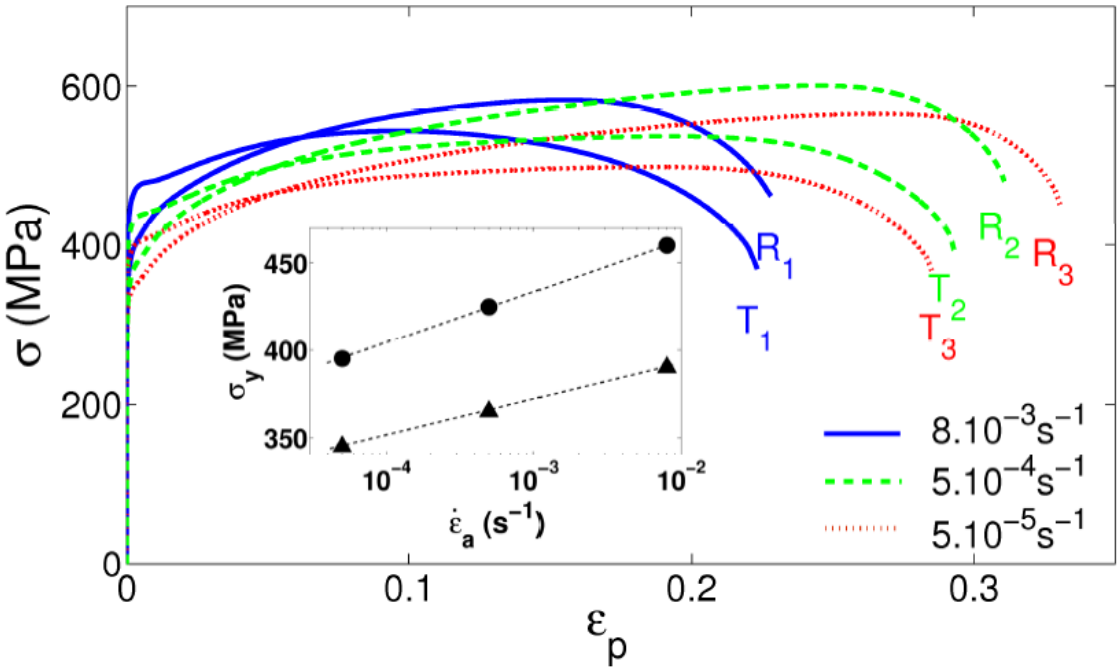

Fig.1. *True stress versus true strain tensile curves of RD and TD-samples at different initial strain rates. Inset: dependence of the yield stress (measured at* $\varepsilon_p = 0.2\%$ *) on the applied strain rate for TD (circles) and RD (triangles) specimens.*

Microstructure analysis. SEM-electron backscatter diffraction (EBSD) method was used to characterize the material microstructure both before and after deformation. The orientation maps were constructed with 0.25 μm step intervals using an HKL Channel5 EBSD system on a JEOL JSM-6490 SEM. The initial texture is typical of rolled Ti [10] with basal planes tilted 30±10° from the normal toward the transverse direction. Fig.2 presents histograms of Schmid factor values for three <a> slip modes: prismatic, basal, and pyramidal, which are expected to be much softer than <c+a> slip. In Ti, prismatic slip is commonly considered as the easiest one. It can be seen that the initial texture of RD-samples is favorable for prismatic and pyramidal <a> glide but precludes basal slip. A different situation is found in the case of TD-samples with much less grains favorably oriented for prismatic glide. The EBSD characterization allowed also for identification of twins. Post-mortem analyses revealed only $\{10\bar{1}2\}\langle\bar{1}011\rangle$T1 tension twins in TD-specimens and mainly $\{11\bar{2}2\}\langle11\bar{2}\bar{3}\rangle$compression C twins in RD-samples but also some minor T1 twins, sometimes inside the C twins.

These observations are consistent with the material texture and the induced solicitation of the c axis. The twin volume fraction was estimated by the intercept method and yielded values between 2.6% and 5.7% for TD-samples. RD-specimens showed an even smaller amount of twins with a total twin volume fraction always less than 0.5%.

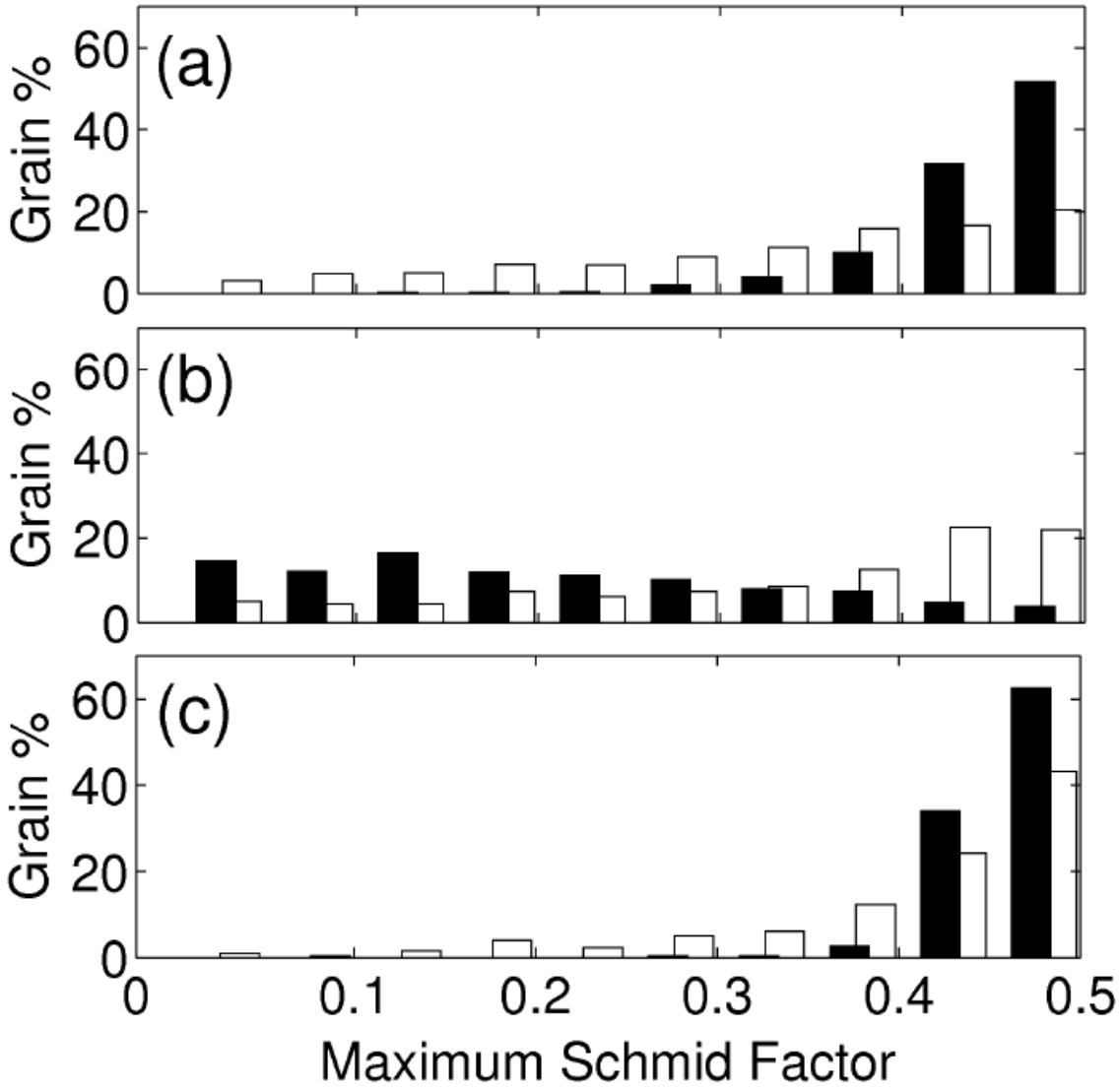

Fig.2. *Distribution of maximum Schmid factors in grains computed from an EBSD map of an undeformed sample for (a) prismatic, (b) basal, and (c) pyramidal <a> slip systems. Solid bars refer to RD, open bars to TD-samples. The analysis is performed on a 984 x 736 μm^2 area covering more than 600 grains.*

Evolution of the strain hardening rate. The shapes of the deformation curves (Fig.1) testify that the three-stage character of deformation of Ti manifests itself in tensile conditions too, although in a less pronounced manner with regard to compression data. Indeed, all deformation curves obtained for TD-specimens show a rather flat region after the elastoplastic transition, followed by a steeper stress increase. These features are emphasized in the consideration of the work hardening behavior as a function of the flow stress (Fig.3). It can be seen that the dependencies obtained for TD specimens present qualitatively the same features as usually reported for compression conditions [6,7], namely, a local minimum followed by a maximum, which marks the boundaries between stage A/stage B and stage B/stage C. The above-described effect of the applied strain rate is expressed by the depth of the well formed by the minimum and maximum, which becomes progressively shallower when $\dot{\varepsilon}_a$ is decreased. Wells are also found for RD-specimens except for the one deformed at the highest strain-rate which displays however a sharp bend followed by an inflection point. The most

striking feature is that the strain-rate effect on the well depth is opposite for the two orientations. Indeed, in contrast to TD-samples, the wells become deeper when the strain rate is decreased in the case of RD-specimens (Fig.3). Another unexpected observation concerns the magnitudes of Θ for two specimen orientations. Fig.3 clearly reveals that after the elastoplastic transition, Θ_R is distinctly higher than Θ_T for all strain-rate values. Plotting Θ as a function of ε_p (not shown), it is observed that the curves go virtually parallel for two orientations after passing their maximum, thus indicating the same plasticity mechanism in both cases.

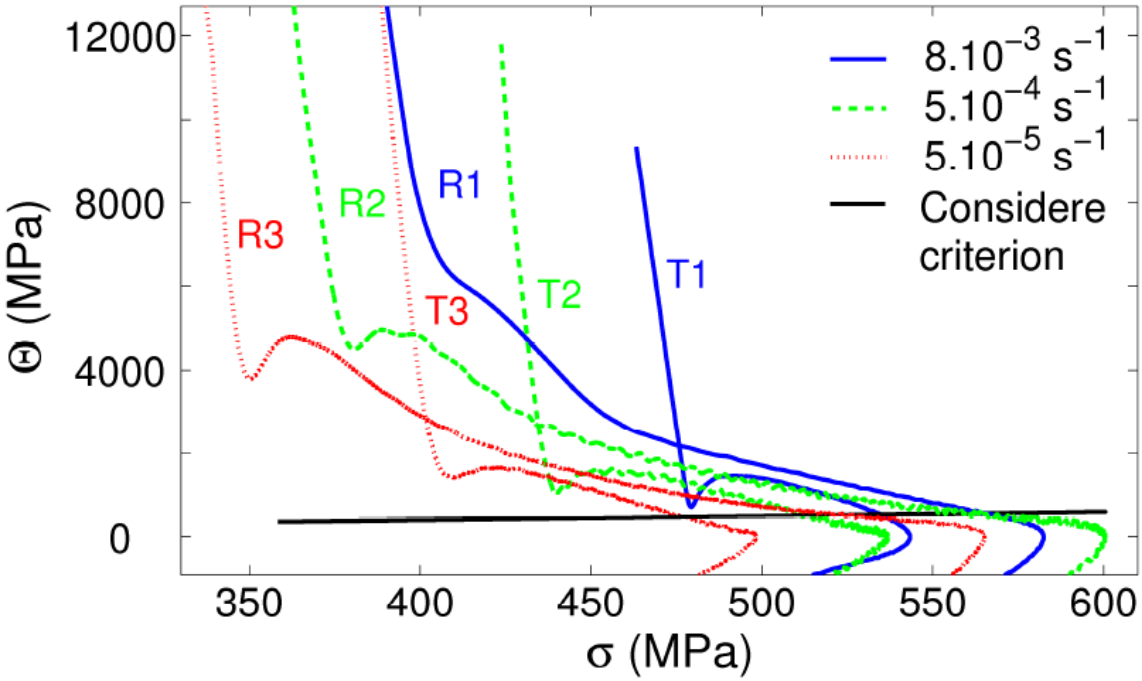

Fig.3. *Initial portions of the curves demonstrating the evolution of the strain hardening rate as a function of flow stress for both RD and TD-specimens at different strain rates.*

Local behavior of plastic strain. Local strain-rate patterns were built using the optical extensometry technique described in detail in [10]. Briefly, it consists in recording the axial positions of about 20 transitions between black and white marks during the sample deformation, using a CCD camera with a recording frequency of 10^3 Hz and a pixel size of 1.3 μm. Fig.4 presents a comparison of the tensile curve and the results of local extensometry for a TD-sample deformed at $\dot{\varepsilon}_a = 8\times10^{-3}$ s^{-1}, i.e., under conditions when the plateau on the deformation curve is rather pronounced. It can be seen that the evolution of the local strain rates displays a global trend correlating with the deformation curve, and also variations on a smaller scale. Importantly, the global trend is similar for all local extensometers. This is particularly clear in Fig. 6(b), which shows no plastic front propagation, but a quasi-simultaneous onset of plasticity over the entire field of vision of the CCD camera. This observation invalidates the conjecture of the occurrence of a propagating Lüders-type band, which could have been made from the observation of a plateau on the applied stress. Moreover, local behavior remains quite homogeneous until necking, which is manifested by a fan-like divergence of local strain-rate curves in Fig. 6(c) and localization of plastic flow at the top of Fig. 6(b). Similar global behavior was observed for all tested specimens, thus

testifying that the occurrence of the low-Θ stage A cannot be ascribed to strain heterogeneity in the form of a propagating deformation band.

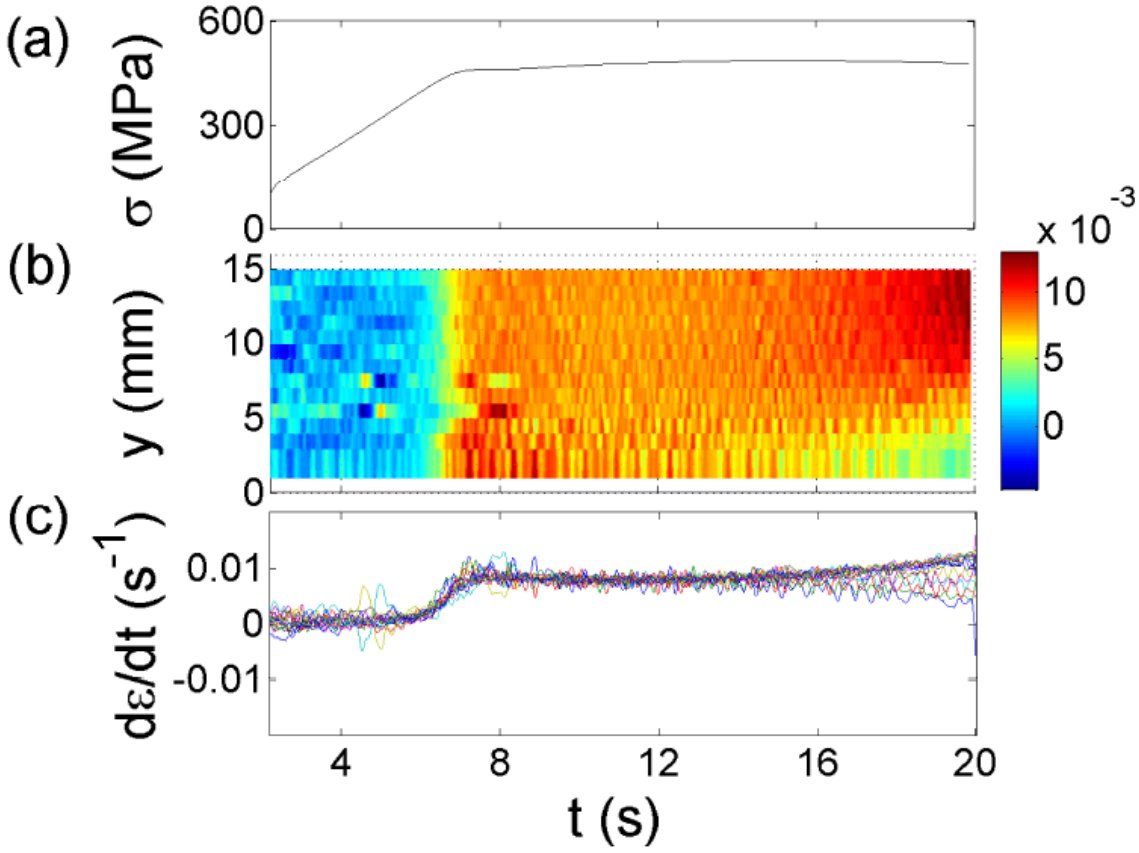

Fig.4. *(a) Portion of an engineering tensile curve for a TD-specimen deformed at* $\dot{\varepsilon}_a$ *=8×10⁻³ s⁻¹; (b) Time–space–local strain rate map obtained using denoising by running average over 100 data points. Some over averaging is used to emphasize the slow global trend. The color bar displays the strain rate scale (s-1); (c) Evolution of the local strain rate for all extensometers.*

Kocks-Mecking modeling

As a first approach, a Kocks-Mecking model [12] that considers the dislocation density r as the governing internal variable was used to describe the observed strain hardening behaviors. Together with a classical power-law kinetic equation, the following evolution equation for r was adopted

$$d\rho / d\varepsilon^p = M\left(k + k_1\sqrt{\rho} - k_2\rho\right) \qquad (1)$$

where *M* is the Taylor factor. *k* and 1 *k* represent the dislocations storage due, respectively, to interactions with grain boundaries and forest dislocations, whereas 2 *k* accounts for dislocations annihilation during the dynamic recovery process. This simplified model is useless to interpret stages A and B since its constitutive equations inevitably lead to a monotonic decrease of Q. However, it proved efficient in describing the strain hardening behavior of our samples during stage C by considering different values of parameters *M* and 1 *k* for RD and TD-specimens (not shown).

Discussion and conclusions

The observation of the parallel course of the $\Theta(\varepsilon_p)$ curves during stage C provides a direct proof for the generally accepted suggestion that even in heavily twinned materials, the dislocations provide the main contribution to strain. This conclusion is also confirmed by the capacity of a simple dislocation-based modeling to retrieve accurately stage C and by the yield stress dependencies on the imposed strain rate, which show behavior characteristic of thermally activated processes (Fig.1). At the same time, the details of work hardening behavior impose a revision of various conjectures described in the Introduction. First, the results of the local extensometry prove that the initial low work hardening rate cannot be ascribed to Piobert-Lüders phenomenon which is caused by solute aging of dislocations. From the first view, the stronger trend to three-stage behavior and the more intense twinning in TD-samples are consistent with the conjecture in [6,7] that such behavior is due to the hardening effect of twins, which is supposed to be responsible for the abrupt Θ increase indicating the onset of the stage B. This hardening effect is ascribed to a dynamic Hall- Petch effect, which considers twin boundaries as obstacles to dislocation glide. However, the hardening conjecture is invalidated by the relationship $\Theta_T < \Theta_R$ which is relevant for all strains (Fig.3). It is known that twins may also produce a softening effect through lattice reorientation favoring dislocation glide within twins. Nevertheless, the observed twin volume fraction is hardly enough to explain the high value of the softening effect whereas the relationship $\Theta_T < \Theta_R$ holds even before stage B, i.e., before the suggested onset of twinning. Finally, the supposed effects of twins do not explain the observed inversion of the sign of the strain-rate effect on the three-stage work hardening, with regard to the orientation of the tensile axis. It is thus probable that twins play a secondary role in tensile deformation of both kinds of specimens.

Since the present data do not support the conjecture of either twinning or dislocation ageing as the mechanisms controlling the RD/TD anisotropy and the three-stage strain hardening, it is of interest to examine the possibility of alternative mechanisms based on dislocation glide only. From Fig.2, it is rather probable that prismatic slip dominates at the beginning of plastic deformation in RD-specimens. This assumption is consistent with the low yield stress and the tendency to “easy glide” (low Θ value) after the elastoplastic transition, the latter observed at the low strain rate.

Various hypotheses may be proposed to explain the influence of $\dot{\varepsilon}_a$ on stage A. The opposite signs of this effect for two kinds of specimens may be taken into account by suggesting that the strain rate sensitivity of stress is stronger for prismatic than for pyramidal glide. Indeed, since this hypothesis means that the stress required for prismatic slip grows stronger than for pyramidal slip when $\dot{\varepsilon}_a$ is increased, it implies a higher contribution of the second (pyramidal) slip system to the plastic flow and, therefore, suppression of “easy glide”. In TD-samples, most of grains are favorable for pyramidal slip (Fig.2), which explains their higher yield stress. At the same time, the fraction of grains that have high Schmid factor values for prismatic and basal slip is also large enough. Consequently, these systems can be active from the very beginning of plastic flow, and the tendency to “easy glide” must be weak. Such behavior corresponds to the observations at the low strain rate. Further, in the framework of the above hypothesis, the domination of the pyramidal slip will be reinforced with an increase in $\dot{\varepsilon}_a$ and “easy glide” will be accentuated, as observed experimentally. The inversion of the

sign of the strain-rate effect thus follows from the selection of dominant glide systems, which is controlled by the material texture and the relative orientation of the tensile axis. In conclusion, the present experimental investigation allows for a conjecture that the peculiar three-stage character of strain hardening of Ti and its alloys might be due to various reasons. Whereas the twinning mechanism seems preponderant in compression at room temperature [6,7], and aging effects may come to the first plan either at higher temperatures [4], these phenomena are unable to explain the presence of similar behavior in tension of CP-Ti at room temperature. A hypothesis is made that such behavior may be due to highly anisotropic nature of dislocation glide. In some sense, the occurrence of stage A is an analogue of easy glide (stage I) in single crystals, which is followed by work hardening due to activation of additional slip systems, as suggested in [3]. Verification of this hypothesis will require a systematic investigation of slip systems activity in two kinds of Ti samples, especially at the transitions between different hardening stages. Besides, more relevant modeling is needed that should take into account different evolutions of dislocation density on slip system families which might have different strain-rate sensitivity.

Acknowledgments

This work was supported by the French State through the program "Investment in the future" operated by the National Research Agency (ANR) and referenced by ANR-11-LABX-0008-01 (LabEx DAMAS), and through the ANR project PHIRCILE (ANR 2010 JCJC 0914 01).

References

[1] J. Jiang, A. Godfrey, W. Liu, Q. Liu, Microtexture evolution via deformation twinning and slip during compression of magnesium alloy AZ31, Mater. Sci. Eng. A 483-484 (2008) 576-579.

[2] D.R. Chichili, K.T. Ramesh, K.J. Hemker, The high-strain rate response of alpha-titanium: experiments, deformation mechanisms and modeling, Acta Mater. 46 (1998) 1025-1043.

[3] S.V. Kailas, Y.V.R.K. Prasad, S.K. Biswas, Influence of initial texture on the microstructural instabilities during compression of commercial a-titanium at 25°C to 400°C, Metall. Mater. Trans. A 25 (1994) 1425-1434.

[4] S. Nemat-Nasser, W.G. Guo, J.Y. Cheng, Mechanical properties and deformation mechanisms of a commercially pure titanium, Acta Mater. 47 (1999) 3705-3720.

[5] M. Doner, H. Conrad, Deformation mechanisms in commercial Ti-50A (0.5 at pct oeq) et intermediate and high-temperatures (0.3 - 0.6 TM), Metall. Trans. 4 (1973) 2809-2817.

[6] A.A. Salem, S.R. Kalidindi, R.D. Doherty, Strain hardening regimes and microstructure evolution during large strain compression of high purity titanium, Scr. Mater. 46 (2002) 419-423.

[7] A.A. Salem, S.R. Kalidindi, R.D. Doherty, Strain hardening of titanium: role of deformation twinning, Acta Mater. 51 (2003) 4225-4237.

[8] L. Bao, J.S. Lecomte, C. Schuman, M.J. Philippe, X. Zhao, C. Esling, Study of plastic deformation in hexagonal metals by interrupted in-situ EBSD measurement, Adv. Eng. Mater. 12 (2010) 1053-1059.

[9] Y.N. Wang, J.C. Huang, Texture analysis in hexagonal materials, Mater. Chem. Phys. 81 (2003) 11-26.

[10] T.A. Lebedkina, M.A. Lebyodkin, J.P. Château, A. Jacques, S. Allain, On the mechanism of unstable plastic flow in an austenitic FeMnC TWIP steel, Mat. Sci. Eng. A 519 (2009) 147-154.

[11] H. Mecking, U.F. Kocks, Kinetics of flow and strain hardening, Acta Metall. 29 (1981) 1865– 1877.